Heterogeneity in ATP-dependent acidification in endocytic vesicles from kidney proximal tubule

Measurement of pH in individual endocytic vesicles in a cell-free system

Lan-Bo Shi, Kiyohide Fushimi, Hae-Rahn Bae, and A. S. Verkman

Departments of Medicine and Physiology, Cardiovascular Research Institute, University of California, San Francisco, California 94143–0532 USA

ABSTRACT Measurement of membrane transport in suspensions of isolated membrane vesicles provides averaged information over a potentially very heterogeneous vesicle population. To examine the regulatory mechanisms for ATP-dependent acidification, methodology was developed to measure pH in *individual* endocytic vesicles. Endocytic vesicles from proximal tubule apical membrane of rat kidney were labeled in vivo by intravenous infusion of FITC-dextran (9 kD); a microsomal fraction was obtained from dissected renal cortex by homogenization and differential centrifugation. Vesicles were immobilized on a polylysine coated coverglass and imaged at high magnification by a silicon intensified target camera. ATP-dependent acidification was not influenced by endosome immobilization. Endosome pH was determined from the integrated fluorescence intensity of individual labeled vesicles after background subtraction. Calibration studies with high K and nigericin showed nearly identical fluorescence vs. pH curves for different endosomes with a standard deviation for a single pH measurement in a single endosome of ~0.2 pH units. In response to addition of 1 mM MgATP in the presence of K and valinomycin, endosome pH decreased from 7.2 to a mean of 6.4 with a unimodal distribution with width at half-maximum of ~1 pH unit. The drop in endosome pH increased and the shape of the distribution changed when the time between FITC-dextran infusion and kidney removal was increased from 5 to 20 min. Differences in ATP-dependent acidification could not be attributed to heterogeneity in passive proton conductance. These results establish a direct method to measure pH in single endocytic vesicles and demonstrate remarkable heterogeneity in ATP-dependent acidification which was interpreted in terms of heterogeneity in the number and/or activity of proton pumps at serial stages of endocytosis.

INTRODUCTION

The apical membrane of kidney proximal tubule undergoes rapid turnover by a cycle of membrane insertion and endocytic retrieval (Rodman et al., 1986; Park, 1988). Endocytic vesicles from rat and rabbit proximal tubule contain functional water channels and proton pumps, but selectively exclude Na-dependent proton and glucose transporters known to be present on proximal tubule apical membrane (Ye et al., 1989). Transport studies in isolated endocytic vesicles have been performed on heterogeneous vesicle populations (Ohkuma et al., 1982; Galloway et al., 1988; Sabolic and Burkhardt, 1986, 1988; Gruenberg and Howell, 1989) and therefore represent averaged transport characteristics. However, based on a substantial body of evidence in a number of cultured cell systems, it is likely that both the qualitative and quantitative membrane transport properties of endocytic vesicles depend strongly upon the stage of endocytosis (Mellman et al., 1986; Roederer et al., 1987; Yamashiro and Maxfield, 1987*a*). Selective sorting of fluid and lipid phase markers, regulatory mechanisms that act only within a brief time window, and membrane fusion and budding processes cannot be examined from averaged data on mixed vesicle populations.

There are several mechanisms by which the rate of endosome acidification and the steady-state endosome pH could be regulated. The rate of acidification depends upon the number and activity of proton pumps, the movement of counterions (cation efflux, and/or anion influx), the membrane potential, and the passive proton conductance (Xie et al., 1983; Mellman et al., 1986; Van Dyke, 1988; Fuchs et al., 1989*a*). In CHO fibroblasts, there is evidence that acidification of early endosomes is regulated by a positive interior membrane potential generated by a ouabain-sensitive 3Na-2K pump (Fuchs et al., 1989*b*; Cain et al., 1989). In endosomes from rabbit kidney, a chloride channel has been identified which is activated by protein kinase A-dependent phosphorylation (Bae and Verkman, 1990). In contrast to the rate of acidification, the steady-state endosome pH would depend more upon the number/activity of proton pumps and the proton conductance than upon the permeability of counterions. There has been no direct experimental evidence to demonstrate the existence of heterogeneity in the activity of proton pumps or the passive proton conductance in endocytic vesicles. Be-

Address editorial correspondence and reprint requests to Dr. A. S. Verkman, 1065 Health Sciences East Tower, Cardiovascular Research Institute, University of California, San Francisco, CA 94143-0532.

0006-3495/91/06/1208/10 $2.00

cause fusion events between early endosomes and more acidic intracellular vesicles occur, it is possible that the number of proton pumps might vary considerably among endosomes. It is more difficult to devise a scheme by which passive proton conductance could be regulated, particularly because regulated proton channels have not been demonstrated in biological membranes.

We describe here the measurement of ATP-dependent acidification in individual isolated endocytic vesicles from rat proximal tubule. The goal of these studies was to determine whether ATP-dependent acidification was heterogeneous and whether the differences in acidification were attributed to differences in the number/activity of functional proton pumps or the magnitude of passive proton conductance. Experiments on isolated endosomes in a cell-free preparation are required to address this question because ion conductances and pump activities are uncertain in endocytic vesicles in the intact cell. In isolated vesicles, the membrane potential can be clamped by use of K and valinomycin so that acidification depends only on proton pump activity and passive proton conductance. Fluorescently labeled endocytic vesicles were immobilized on a glass coverslip in a perfusion chamber for measurement of pH by quantitative fluorescence microscopy. From pH calibrations performed in single endosomes, measurement of pH to within 0.2 units was possible. pH distributions were obtained by imaging many endocytic vesicles simultaneously. The influence of endosome size and stage on the pH distribution was examined. The methodology described here should have general applications to the study of transport heterogeneity by fluorescence in isolated membrane vesicles or subcellular fractions.

METHODS

Endosome isolation

Female Sprague-Dawley rats (200–250 g) were infused over 1 min with 2 ml of phosphate-buffered saline containing 50 mg FITC-dextran (9 kDa, Sigma Chemical Co., St. Louis, MO, dialyzed for >24 h to remove unconjugated FITC). After 5 or 20 min, the rat was sacrificed and the aorta was perfused with 30 ml of 100 mM KCl, 2 mM $MgCl_2$, 100 mM mannitol, 5 mM K phosphate, pH 7.5, 0–2°C (buffer A). All subsequent procedures are carried out at 0–2°C. The renal cortex (0.5 mm depth) was dissected and homogenized with 5 strokes of a Dounce homogenizer and 10 strokes of a Potter-Elvehjem homogenizer. The suspension was centrifuged at 750 *g* for 10 min to remove debris and 5,000 *g* for 10 min to remove mitochondria, lysosomes, and heavy vesicles. The supernatant was centrifuged at 100,000 *g* for 30 min to produce a microsomal pellet containing the labeled endocytic vesicles. Microsomes were washed once with 40 ml of buffer A and homogenized with five passages through 23 and 26 gauge steel needles. The average membrane yield was ~0.2 mg microsomal protein per kidney. Microsomes were maintained at 0–2°C at a concentration of 2–4 mg protein/ml for <2 h. The concentration of serum FITC was estimated from the fluorescence of a 1,000-fold dilution of a blood sample obtained at the time of kidney removal.

Liposome preparation

Liposomes containing 6-carboxyfluorescein (6CF) were prepared by extrusion through 0.22 μ Millipore filters. A mixture of 95% phosphatidylcholine, 5% phosphatidylserine was dried under N_2 and suspended in buffer A containing 0.1 mM 6CF at a concentration of 10 mg lipid/ml. The suspension was extruded 10 times through two 0.22 μ filters in series under high pressure to give a uniform population of liposomes of diameter 0.2–0.25 μ (Verkman et al., 1989*a*). External 6CF was removed by Sephadex exclusion chromatography.

Fluorescence microscopy measurements

Glass coverslips (0.11 mm thickness) were washed with spectroscopic grade acetone and ethanol, and coated with 0.5 ml of 0.01% poly-*l*-lysine by incubation for 30 min at 23°C. To immobilize endocytic vesicles, 50 μl of a dilute microsomal suspension (0.5 mg/ml) containing anti-FITC antibody (50–100 mU/ml; Molecular Probes, Junction City, OR) was incubated for 15 min with the poly-*l*-lysine coated coverslip at 23°C in a moisturized chamber. The coverslip was gently washed with buffer A and mounted in a laminar flow perfusion chamber consisting of a 2 mm wide fluid channel bounded on top by a glass coverslip and on the bottom by the coverslip with vesicles facing upward. Solutions bathing the vesicles were perfused continuously at 3–5 ml/min to give exchange times of under 0.2 s (Chao et al., 1989). All solutions were bubbled for >30 min with N_2 to minimize oxygen-dependent photobleaching of FITC.

Endosomes were viewed on a Nikon inverted epifluorescence microscope (Diaphot) with 100× fluortar objective (oil immersion, N.A. 1.30, working distance 0.17 mm). Fluorescence was excited at 495 nm by a 100 W stabilized tungsten-halogen light source, KG-3 red blocking filter, OD 1 neutral density filter, 495 ± 5 six-cavity interference filter (Omega Optical, Brattleboro, VT), and 510 nm dichroic mirror. Emitted light was filtered by KV505 and OG515 cut-on filters (Schott Glass, Duryea, PA) and 512 × 480 × 8 bit images were acquired by a silicon intensified target camera (model SIT-66; DAGE-MTI, Michigan City, IN) operating at fixed gain using image acquisition hardware from Data Translation Inc. (Marlboro, MA). Generally 25–50 frames (~5 s) were averaged to obtain a single image. Histograms of pixel intensity were examined in every image to confirm that intensities were in the linear region of the camera response as described previously (Fushimi et al., 1990). The shutter was opened only during the data acquisition to minimize photobleaching.

Image analysis

Computer software was written in Microsoft C to determine endosome intensities for a series of images using an approach similar to that adopted by Dunn et al. (1989) in intact cell studies. There were generally 10–25 labeled endocytic vesicles per 80 × 80 μ visual field. A square measuring box (generally 2 × 2 μ) was automatically centered to the peak pixel intensity in each endocytic vesicle. The area-integrated intensity was calculated and corrected for background. The local background signal was determined from the average pixel intensity in the annular region between the square measuring box and a concentric larger box (generally 4 × 4 μ). For background subtraction, an area-integrated background was calculated from the product of the local background signal per pixel and the number of pixels in the smaller measuring box. Integrated intensities were determined for

each endocytic vesicle in a series of images. The time course of absolute or relative fluorescence intensity for individual endocytic vesicles could be displayed and averaged, or pH could be calculated and correlated with intensity. Absolute vesicle fluorescence was expressed as the integrated pixel intensity after subtraction of background. Relative fluorescence was calculated to compare data for vesicles of differing brightness. Relative fluorescence was determined by multiplication of absolute intensities by factors determined to minimize the deviations in y values of each curve from the average curve. pH values were calculated from relative intensities and the relative intensity vs. pH calibration relation (Fig. 3) after correcting intensities for photobleaching (3–6%/intensity measurement, see below).

Cuvette fluorimetry measurements

Measurements of ATP-dependent acidification were made of microsomal vesicles in suspension (10–20 μg protein/ml) or immobilized on a 9 × 22 mm rectangular glass coverslip positioned at an angle of 30° from the incident light. To initiate inward proton pumping, 1 mM ATP (stock 100 mM ATP titrated to pH 7.5) was added to 2 ml of buffer A in an acrylic cuvette at 23°C. The time course of FITC-dextran fluorescence (excitation 495 nm, emission >515 nm) was measured continuously and averaged over 1-s time intervals. After endosomal pH reached a steady-state level, the pH gradient was collapsed by addition of 5 μM nigericin. Absolute endosomal pH was calculated from the fluorescence vs. pH relation and the endosomal FITC-dextran signal determined by addition of the anti-FITC antibody to quench external fluorescence (Ye et al., 1989).

RESULTS

The optimal conditions for immobilization and visualization of individual endocytic vesicles labeled with FITC-dextran were first determined. A microsomal suspension containing the in vivo-labeled endocytic vesicles was immobilized on a poly-*l*-lysine coated glass coverslip. The coverslip was washed and mounted in a perfusion chamber in which fluorescence was measured by short working distance objectives with high numerical aperture.

Fig. 1 (*top*) shows images of labeled endocytic vesicles in buffer A at pH 7.5 (*left*) and 6.5 (*right*). To immobilize 15–25 labeled vesicles in a 80 × 80 μ square microscope field, coverslips coated with 0.01% poly-*l*-lysine were incubated with the microsome suspension. A low poly-*l*-lysine concentration was used to minimize background signal. Preincubation of microsomes with the anti-FITC antibody decreased background further by quenching the fluorescence of externally bound or aqueous FITC-dextran. The figures show ~15 well-demarcated labeled vesicles whose fluorescence is pH dependent.

The majority of vesicles are below the size resolution of the light microscope and therefore appear as circular diffraction patterns (Airy disks) whose diameter depends upon wavelength and objective numerical aperture (Inoue, 1989). Fig. 1 (*middle, left*) shows an expanded image of a single endocytic vesicle. The intensity profile across a single vesicle (averaged over 10 vesicles) is shown in Fig. 1 (*middle, right*); the width at half-maximum is ~0.6 μ. Fig. 1 (*bottom, left*) shows the field of vesicles given in Fig. 1 (*top*) together with measuring boxes. The inner measuring box was used to integrate the total fluorescence intensity of an individual endocytic vesicle. Background signal was determined from the average pixel intensity between the inner and outer boxes. The arrow denotes two closely spaced endocytic vesicles that were not included in the analysis because background signal could not be determined unambiguously.

Experiments were carried out to evaluate the smallest number of entrapped fluorescein molecules that could be visualized. Liposomes containing 0.1 mM 6CF were immobilized on coated coverslips and imaged at high camera gain. 6CF and FITC have similar molar absorbance and quantum yield. Fig. 1 (*bottom, right*) shows that individual 0.2–0.25 μ liposomes containing 0.1 mM 6CF could be visualized. There are ~35 molecules of 6CF entrapped in one liposome. From measurements of FITC fluorescence in rat blood, an individual endocytic vesicle of 150 nm diameter would contain 100–150 FITC molecules. Therefore, it is possible to visualize single labeled endocytic vesicles.

Control experiments were performed to determine whether the immobilization of endocytic vesicles by poly-*l*-lysine influenced ATP-dependent acidification. Experiments were performed by cuvette fluorimetry, comparing acidification in a stirred suspension and immobilized population of microsomes (Fig. 2). ATP addition caused a prompt fluorescence decrease due to inward proton pumping. The decrease in fluorescence was reversed by addition of the K/H ionophore nigericin. Both the steady-state pH attained after 2 min (6.3 ± 0.1, suspension; 6.35 ± 0.1, immobilized vesicles; SD, n = 3) and the initial rate of acidification (0.08 ± 0.01 pH units/s, suspension; 0.07 ± 0.01 pH units/s, immobilized vesicles) were not influenced by immobilization. These results also support the view that the immobilized endocytic vesicles represent a random rather than a selected sample of the total vesicle population.

Measurements of pH in individual endocytic vesicles were performed by quantitative imaging microscopy. The first set of studies was designed to examine measurement accuracy, photobleaching effects, pH calibration, and volume dependence of fluorescence. Fig. 3 shows a pH calibration experiment in which the perfusion solution contained nigericin and high K to equilibrate intravesicular and solution pH rapidly. Measurements (Fig. 3; *at arrows*) were made 1 min after perfusion with solutions at the indicated pH. Vesicle intensity changed within 10 s and was stable after 30 s in response to a

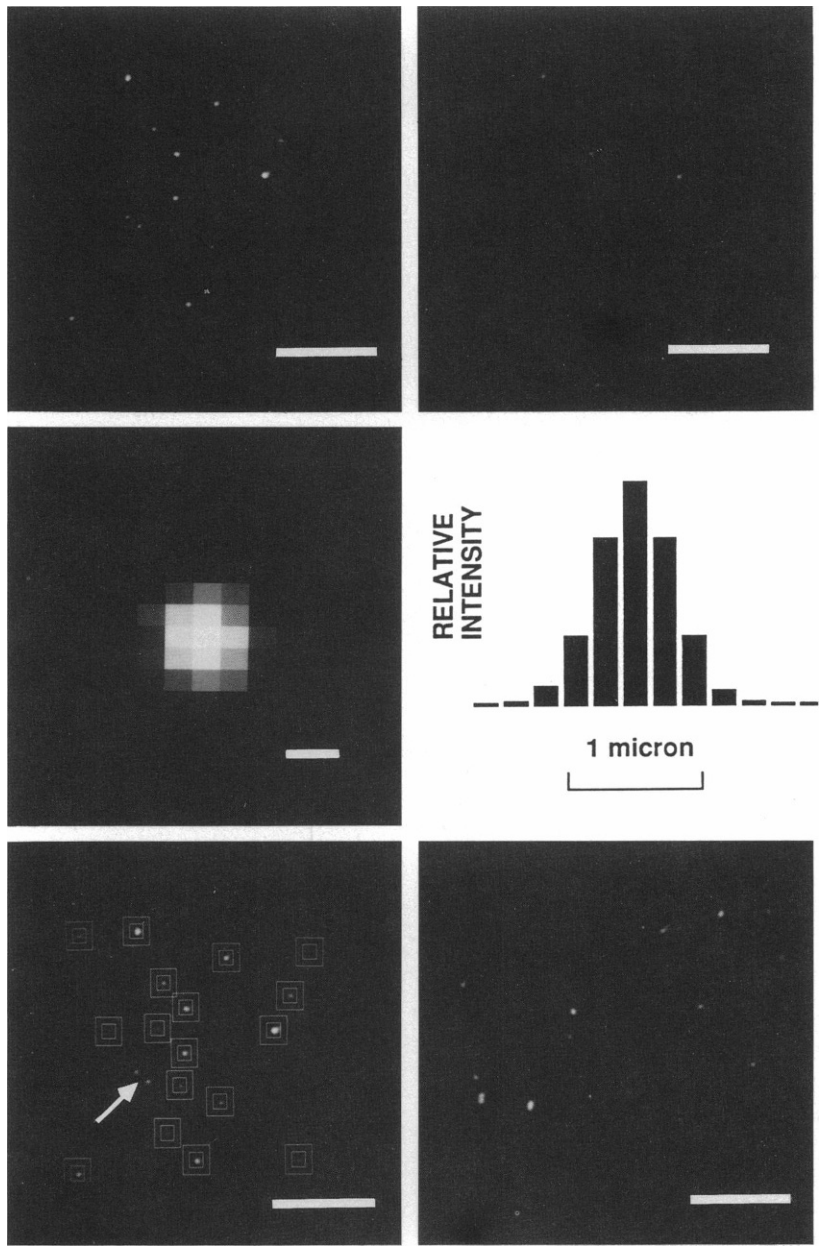

FIGURE 1 *Top:* Images of endocytic vesicles from rat proximal tubule labeled with FITC-dextran and immobilized on a poly-*l*-lysine coated glass coverslip. The pH of perfusion solutions was 7.5 (*left*) and 6.5 (*right*). Labeled vesicles were imaged by a SIT camera through a 100× objective (N.A. 1.3) as described in Methods. Excitation wavelength was 495 nm with emission at >515 nm. Scale bar 16 μ. *Middle:* Expanded view of a single endocytic vesicle with intensity profile across vesicle. Scale bar 0.5 μ. *Bottom* (*left*): the same microscope field as in *top* (*left*) with square measuring boxes. The arrow points to two vesicles which were excluded from analysis because of their proximity (see text). *Bottom* (*right*): image of 0.2–0.25 μ diameter liposomes containing 0.1 mM 6-CF. Scale bar 16 μ. All measurements were performed at 23°C.

change in pH of the perfusion solution. There was wide variation in the absolute pixel intensities of individual labeled vesicles (Fig. 3 *A*) due to differences in vesicle size and, possibly, to the intravesicular concentration of FITC-dextran. To facilitate the comparison of fluorescence vs. pH, Fig. 3 *B* shows a plot of the same data with relative intensity plotted on the ordinate. The data were not corrected for photobleaching (see below). The relationship between relative integrated intensity and pH was not systematically different in separate endocytic vesicles and did not correlate with vesicle size.

The intensity at pH 8.5 at the end of the experiment

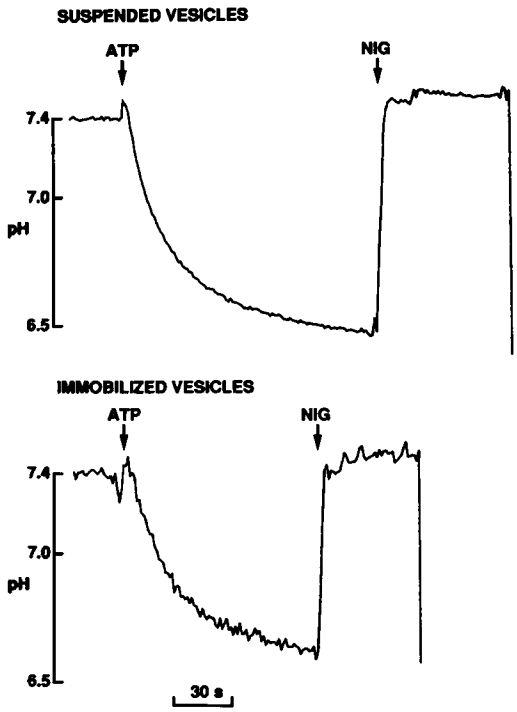

FIGURE 2 ATP-dependent acidification in suspended and immobilized endocytic vesicles measured by cuvette fluorimetry. Kidneys were removed 20 min after FITC-dextran infusion. A microsomal suspension containing FITC-dextran labeled endocytic vesicles was used in both experiments. Where indicated, 1 mM ATP and 5 μM nigericin were added.

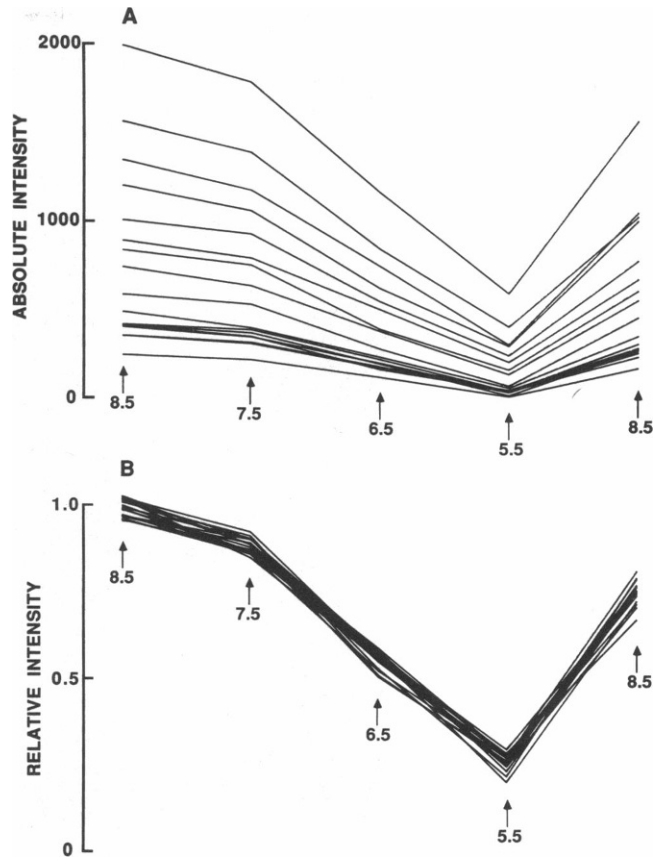

FIGURE 3 Calibration of fluorescence vs. pH for individual labeled endocytic vesicles. Vesicles were perfused continuously with buffer A containing 5 μM nigericin and titrated with NaOH or HCl to pH 5.5, 6.5, 7.5, and 8.5. Images were acquired after a 1 min perfusion with each buffer. Plots of the absolute integrated pixel intensity (*A*) and relative intensity (*B*) are given (see text).

was always less than that at the beginning of the experiment. The possibilities for this difference are photobleaching, dye leakage, and a change in the objective focal plane. For the study in Fig. 3, the illumination shutter was opened for ~6 s for each intensity measurement. Control experiments were performed in which vesicles were perfused with the pH 8.5 buffer. When the shutter was open continuously, the relative intensity decreased at a rate of >40%/min. When the shutter remained closed except for an intensity measurement at 5 min, there was <5% decrease in intensity. Therefore, there was considerable photobleaching at the illumination intensities required for acceptable measurement accuracy, but little leakage of FITC-dextran. There was no systematic effect of vesicle size on leakage rates when vesicles of different intensity were analyzed separately. There was little effect on intensities of changing the objective focal plane to a point where the Airy disk diameter increased by 50%. In the actual experiments there was no change in the focal plane and generally no pixel misregistration in a series of images of the same field. For calculations of pH, photobleaching effects were corrected as described in Methods. The average SD for a series of calibrations performed on 10–20 vesicles on five separate coverslips (total 74 vesicles) was 0.07 relative fluorescence intensity units. In the pH range 6–7.5, this corresponds to a ~0.2 pH unit uncertainty in vesicle pH.

FITC-dextran fluorescence may be sensitive to both pH and to volume if concentration-dependent self-quenching occurs. In the subsequent studies of ATP-dependent acidification, the maximal change in vesicle volume would be much >15%.[1] To investigate the effect

[1]The internal buffer capacity of endocytic vesicles was measured to be ~40 mM/pH unit at pH 6.0–7.5 by the ammonia pulse technique using stopped-flow fluorimetry. For a 1 pH unit decrease, the maximal change in vesicle volume would be <15% if H entry is accompanied by 40 mM K exit. The actual volume change is probably much smaller because some of the H entry would be accompanied by Cl entry.

of a 20% decrease in vesicle volume, 60 mM sucrose was added to the perfusion solution. Average fluorescence decreased by 3 ± 4% (SD, 28 vesicles), indicating little effect of volume change under the experimental conditions.

ATP-dependent acidification in individual endocytic vesicles was evaluated by measurement of intensities before ATP addition, 30 s and 2 min after addition of 1 mM ATP, and after 1 min of perfusion with buffers containing nigericin at pH 8.5 and 5.5. Fig. 4 *A* shows the absolute intensities for a group of vesicles studied on a single microscope slide. As in the calibration experiment, there was considerable variation in individual intensities. The plot of relative intensity (Fig. 4 *B*) shows that most vesicles acidified in response to ATP addition, however the extent of acidification was quite variable. pH values calculated from relative intensities are given in Figs. 5 and 6 below. A similar plot of relative intensity is shown for an experiment in which the proton pump inhibitor *N*-ethylmaleimide (NEM, 0.5 mM) was present in all solutions. Although the statistical variability in signal was similar in Fig. 4 *B* and *C*, there was no systematical acidification of endocytic vesicles in the presence of NEM.

The data for a series of studies on a single preparation of endocytic vesicles typical of three is given in Fig. 5. Vesicles were prepared from kidneys removed at 5 and 20 min after intravenous infusion of FITC-dextran. For each vesicle, the pH measured at 2 min after ATP addition was compared with the absolute intensity before ATP addition, an approximate measure of vesicle size. Although the correlation between vesicle pH and intensity was weak above pH 6.2, the vesicles which attained the lowest pH had relatively low intensities (see Discussion). Plots of vesicle number vs. pH in Fig. 6 show lower pH values, and a wider distribution of pH values, for vesicles prepared from kidneys removed at 20 min compared with 5 min after FITC-dextran infusion. The intensity weighted average pH of the "20 min" vesicles was 6.4, giving an average ATP-dependent pH drop of 0.8 units which is in agreement the whole-population data in Fig. 2. This close agreement provides good evidence that the measurement of ATP-dependent acidification on single vesicles is valid. The intensity weighted average pH for the "5 min" vesicles was 6.6.

Passive proton conductance in individual endocytic vesicles was measured from the time course of acidification in response to a decrease in solution pH in the presence of K and valinomycin. Fig. 7 shows a plot of relative fluorescence vs. time. Images were recorded every 30 s after changing solution pH from 7.4 to 6.5. Qualitatively, there was relatively little variation in

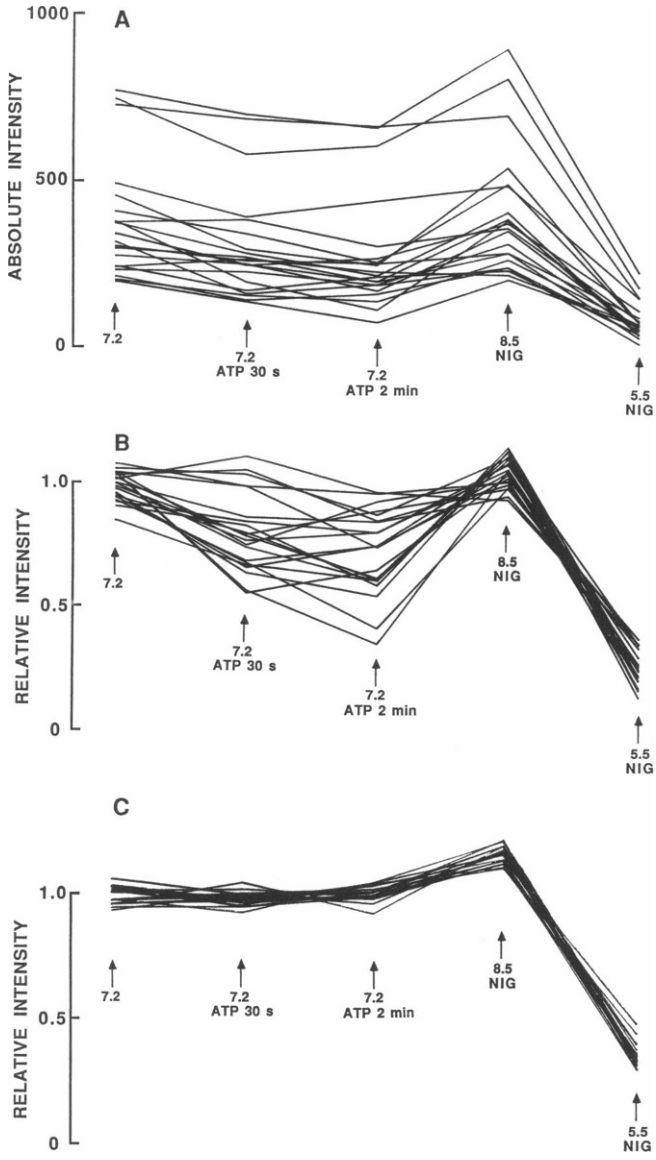

FIGURE 4 ATP-dependent acidification in individual labeled endocytic vesicles. Vesicles were first perfused with buffer A at pH 7.2 in the presence of valinomycin (2 μM). Images were acquired 30 s and 2 min after addition of 1 mM Mg-ATP. Two calibration points were subsequently obtained after 1 min perfusion with buffer A titrated to pH 8.5 and 5.5 in the presence of 5 μM nigericin. Plots of the absolute integrated pixel intensity (*A*) and relative intensity (*B*) for individual vesicles are given. A plot of relative intensity for the same protocol performed in the presence of 0.5 mM *N*-ethylmaleimide shows inhibition of ATP-dependent acidification (*C*). Data shown were not corrected for photobleaching; in this set of experiments, the photobleaching correction was 3.4% for each intensity measurement.

passive proton permeability in individual endocytic vesicles. To estimate the rate of passive proton transport, photobleaching-corrected data for each endosome was fitted to a single exponential function. In 28 separate

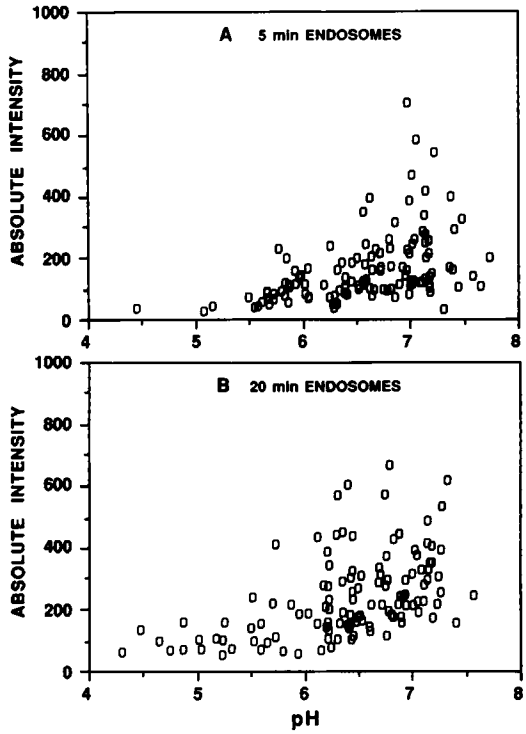

FIGURE 5 Correlation between pH and absolute integrated pixel intensity for a series of labeled endocytic vesicles. Vesicles were isolated from kidneys removed 5 min (*A*) and 20 min (*B*) after intravenous infusion of FITC-dextran. Measurements of ATP-dependent acidification were performed as in Fig. 4. The abscissa is the pH measured at 2 min after ATP addition. The ordinate is the integrated pixel intensity prior to ATP addition.

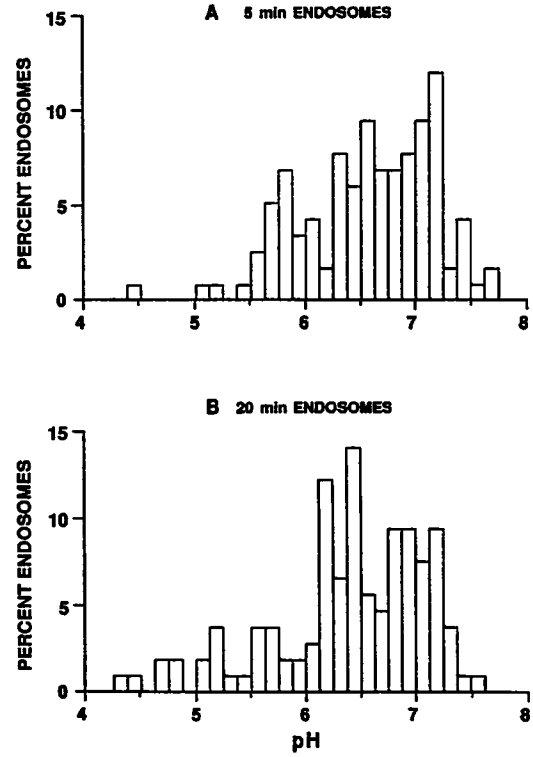

FIGURE 6 Histogram of the percentage of labeled vesicles vs. pH measured at 2 min following addition of ATP. Vesicles were isolated from kidneys removed 5 min (*A*) and 20 min (*B*) after intravenous infusion of FITC-dextran.

endocytic vesicles, the time constant for the pH decrease was 43 ± 8 s (SD).

DISCUSSION

The purpose of this study was to develop methodology to measure pH accurately in individual isolated endocytic vesicles for analysis of heterogeneity in ATP-dependent acidification. Fluorescence activated cell sorting was not a suitable approach for measurement of pH in individual vesicles in a cell-free system because of the small vesicle size (< 180 nm diameter) giving a very small fluorescence signal, and the inability to follow the time course of fluorescence in individual endocytic vesicles. High sensitivity quantitative imaging of immobilized, fluorescently labeled endocytic vesicles was used to measure pH in individual labeled vesicles with ~0.2 pH unit resolution, and to follow the time course of pH in response to addition and removal of effectors. Calibration studies showed similar relative fluorescence vs. pH curves in individual labeled vesicles. Studies of ATP-dependent acidification showed remarkable heterogeneity in the pH response of individual endocytic vesicles from kidney proximal tubule.

Vesicles were immobilized on poly-*l*-lysine coated

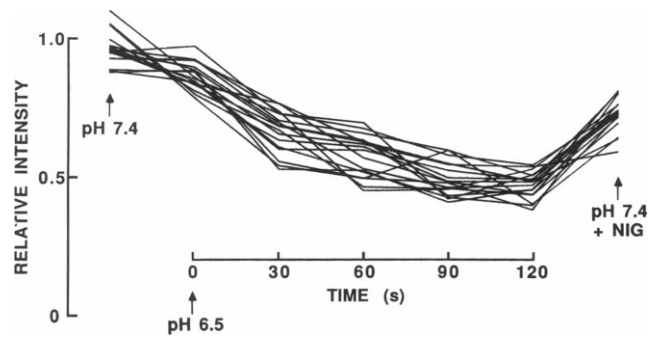

FIGURE 7 Passive proton conductance in individual endocytic vesicles. Vesicles were first perfused with buffer A at pH 7.4 in the presence of 2 μM valinomycin. Where indicated, the pH was decreased to 6.5 to drive inward proton movement. Images were obtained every 30 s for 120 s, and then 1 min after infusion of buffer A at pH 7.4 in the presence of 5 μM nigericin.

coverslips. Poly-*l*-lysine has been used extensively to immobilize cells and cellular fractions in a nonselective manner. The immobilization of endocytic vesicles did not alter their acidification in response to ATP, providing evidence that poly-*l*-lysine did not alter proton pump function nor bind a subpopulation of endocytic vesicles selectively. During the course of a typical 10 min experiment with continuous perfusion, >95% of labeled vesicles remained immobilized and observable.

The fluid-phase marker FITC-dextran (9 kD) was used to label endocytic vesicles. FITC-dextran is freely filtered by the kidney glomerulus and available in the proximal tubule lumen as a fluid-phase marker of endocytosis. It was shown that >95% of endocytic vesicles from rat kidney cortex labeled by the in vivo protocol in these studies originated from the apical membrane of proximal tubule (Lencer et al., 1990*a*). FITC-dextran fluorescence is sensitive to vesicle volume and pH, which has made possible the measurement of osmotic water, solute and ion-coupled proton permeabilities, and ATP-dependent acidification in endocytic vesicles containing the vasopressin-sensitive water channel (Verkman et al., 1988; Shi and Verkman, 1989; Lencer et al., 1990*b*). FITC has good optical properties for use as an endocytic marker including high quantum yield (0.9) and molar absorbance (8×10^4 $M^{-1}cm^{-1}$), and blue/green excitation and emission wavelengths. Fluorophore brightness is particularly important because of the small size of endocytic vesicles; there were only ~120 molecules of FITC in a vesicle of 150 nm diameter labeled in vivo with FITC. Another advantage of FITC is the availability of the anti-FITC antibody, an impermeant, very efficient quencher of extravesicular FITC that is bound nonspecifically to the external vesicle surface or to the positively charged poly-*l*-lysine. Disadvantages of FITC-dextran are a moderately high rate of photobleaching and the inability to measure pH by an excitation ratio method because of the relatively poor signal-to-background at a 450 nm excitation wavelength under the conditions of our experiment. Photobleaching was minimized by removal of solution oxygen and use of low illumination intensity. Pyranine and BCECF-labeled dextran are potentially useful fluid-phase markers for a ratiometric measurement of pH in individual endocytic vesicles in the pH range 6.5–8 (Straubinger et al., 1990).

Quantitation of the spatially integrated intensity of a single endocytic vesicle required the measurement of fluorescence of a particle smaller than the wavelength of light. The general problem of visualizing objects smaller than the resolution limit of the light microscope has been evaluated and mathematically modeled (Inoue, 1989). In fluorescence microscopy, the *x-y* spatial pattern of a very small sphere is described by the Airy disk. For the smallest labeled vesicles, the width at half maximum of the intensity distribution using the 100×, 1.3 N.A. objective was ~0.6 μ. Out-of-focus effects were not important because of the small size and good separation of the labeled vesicles, and because labeled vesicles were strictly in the same focal plane.[2] By choosing the measurement box to be larger than the Airy disk, the integrated intensity was insensitive to the precise objective focus. Slight shifts in the *x-y* position did not influence intensities because of the large size and automatic centering of the measuring box. The determination of a local background signal in a region outside of the Airy disk was important to avoid artifacts from nonuniformity in illumination and camera shading. Data from repeated measurements and from calibration experiments showed that pH in the range 6–7.5 was measurable to ~0.2 units. Therefore, the distribution in pH values in ATP studies represents heterogeneity in acidification rather than instrument artifact.

The distribution of steady-state pH values in endocytic vesicles after ATP addition is broad and complex, revealing information not available from averaged measurements. The distribution is broadened and shifted to lower pH values when the time between FITC-dextran infusion and kidney removal increased from 5 to 20 min. Because serum FITC-dextran concentration remains elevated for >30 min after FITC-dextran infusion, the labeled endocytic vesicles represent a time-integrated population rather than a pulse-labeled cohort. The relatively small variability in passive proton conductance (~20% variability in rates) in labeled vesicles makes it unlikely that acidification is controlled by the magnitude of the passive proton leak; the variability in ATP-dependent pH values was approximately fivefold greater.[3] Therefore, the heterogeneity in acidification is most consistent with heterogeneity in the number and/or activity of functional proton pumps. These results support the view that acidification begins

[2]All labeled vesicles in the visual field were in sharp focus simultaneously. For a maximum vesicle diameter of 1 μm and using the measured point-spread-function for the 100× oil immersion objective, out-of-focus effects would be measurable if vesicles were <3 μm apart.

[3]Under voltage-clamp conditions, the relationship between proton flux and transmembrane pH gradient (ΔpH) can be approximated by the relation, $d[\Delta pH]/dt = -P_H(\Delta pH) + I_{ATP}$, where P_H is passive proton permeability and I_{ATP} is the proton pump activity (Verkman and Alpern, 1987). In the steady-state ($d[\Delta pH]/dt = 0$), $\Delta pH = I_{ATP}/P_H$. Thus, a nonzero width of the pH distribution could be due to heterogeneity in I_{ATP} or P_H. To account for a width of the ΔpH distribution of ~1 pH unit centered at ΔpH = 1 (average pH of 6.3 after ATP addition), there must be nearly 100% heterogeneity in the distributions in I_{ATP} or P_H. Because the width of the P_H distribution is ~20% of its mean, the heterogeneity in ΔpH arises predominantly from heterogeneity in I_{ATP}.

very early after endocytosis, and that acidification is progressive and accompanied by fusion events (Willingham and Pastan, 1984; Mellman et al., 1986; Gruenberg and Howell, 1989). From recent work involving receptor-mediated endocytosis in fibroblasts, it is believed that endocytic vesicles undergo progressive acidification from clathrin-coated vesicles (pH > 6.5) to early endosomes (pH 6–6.5) to late endosomes (prelysosomal vesicles; pH 5.5–6) to lysosomes (pH < 5.5) (Mellman et al., 1986; Yamashiro and Maxfield, 1987*a*, *b*; Roederer et al., 1987). There is relatively little information about the kinetics of acidification in fluid-phase (receptor-independent) endocytosis by epithelial cells.

The density of proton pumps at various stages of endocytosis might be modulated by intracellular membrane fusion and budding events. According to this view, the size of clathrin-coated vesicles (Verkman et al., 1989*b*) and early endosomes is quite small (100–160 nm diameter), whereas that of late endosomes is generally much larger (200–400 nm). The early endosomes are usually located in superficial areas of the cell near the plasma membrane of origin. The acidic late endosomes generally appear as multivesicular bodies in the deeper, perinuclear regions of the cell. Several lines of evidence suggest that the majority of labeled vesicles represent early endosomes: (*a*) morphological studies in tissue sections show that nearly all vesicles labeled with FITC-dextran are located in the subapical region of proximal tubule cells (Lencer et al., 1990*a*). (*b*) The diameter of labeled vesicles was ~150 nm as measured by transmission electron microscopy (Lencer et al., 1990*a*). (*c*) The minimum pH reported here was higher than that expected for late endosomes. In addition, it is likely that lysosomes and multivesicular bodies, if labeled, would be removed in the low speed centrifugations. The conclusion that labeled lysosomes are absent in the microsomal pellet is supported by the lack of GTP-dependent acidification (data not shown). Therefore, we believe that the heterogeneity in ATP-dependent acidification represents differences in the activity and/or number of functional proton pumps at early stages of endocytosis.

It must be cautioned that the general findings reported for receptor-mediated endocytosis in fibroblasts may not apply to fluid-phase endocytosis in epithelial cells. The finding that the vesicles with lowest intensity acidified strongly was not expected from the data in fibroblasts. These results indicate the presence of small endocytic vesicles in proximal tubule cells which acidify strongly in response to ATP. As a further caution in the interpretation of cell-free data in terms of intracellular interactions of endocytic vesicles, recent data suggests that endocytosis may not consist of distinct fusion and budding processes, but rather a continuous endosomal reticulum (Hopkins et al., 1990). Further immunocytochemical and fractionation studies are required to assign the exact cellular origin of vesicles with defined acidification properties.

There are a number of assumptions and potential limitations of the methodology developed here. The low signal intensity of individual endocytic vesicles requires optimal optical and perfusion systems to avoid artificial broadening of pH distributions because of measurement errors. The assumption that integrated fluorescence intensity is related to pH by the same function in every vesicle should be established by direct calibration experiments. The possible immobilization of a selected population of endocytic vesicles must be considered, particularly if vesicle size or physical properties are very heterogeneous. Aggregation of two or more small vesicles in a single Airy disk is possible and may be difficult to evaluate. If the fluid-phase fluorescent marker is slightly permeable, then the smallest vesicles with highest surface-to-volume ratios would leak the marker fastest, leading to a skewed distribution of pH values. Finally, the assumption that the integrated intensity is related to vesicle size must be viewed cautiously because of the uncertain osmotic changes in vesicle volume which occur in cell cytoplasm, and the unknown transfer efficiencies of fluid-phase markers during vesicle fusion events.

Recognizing these limitations, the study of membrane transport in individual isolated vesicles provides important information about intracellular membrane trafficking that is not available from population averages on mixed or fractionated samples. The methodology described here should have applications to the study of functional heterogeneity in a variety of transport processes in isolated biomembrane vesicles.

This work was supported by National Institutes of Health grants DK39354, DK35124 and HL42368, a grant from the National Cystic Fibrosis Foundation and a grant-in-aid from the American Heart Association. Dr. Fushimi was supported by a fellowship from the National Kidney Foundation of Northern California. Dr. Verkman is an established investigator of the American Heart Association.

Received for publication 11 July 1990 and in final form 17 January 1991.

REFERENCES

Bae, H.-R., and A. S. Verkman. 1990. Protein kinase A regulates chloride conductance in endocytic vesicles from proximal tubule. *Nature (Lond.)*. 348:637–639.

Cain, C. C., and R. F. Murphy. 1988. A chloroquine-resistant Swiss 3T3 cell line with a defect in late endocytic acidification. *J. Cell Biol.* 106:269–277.

Cain, C. C., D. M. Sipe, and R. F. Murphy. 1989. Regulation of endocytic pH by the Na^+, K^+-ATPase in living cells. *Proc. Natl. Acad. Sci. USA.* 86:544–548.

Chao, A. C., J. A. Dix, M. Sellers, and A. S. Verkman. 1989. Fluorescence measurement of chloride transport in monolayer cultured cells: mechanisms of chloride transport in fibroblasts. *Biophys. J.* 56:1071–1081.

Dunn, K. W., T. E. McGraw, and F. R. Maxfield. 1989. Iterative fractionation of recycling receptors from lysosomally destined ligands in an early sorting endosome. *J. Cell Biol.* 109:3303–3314.

Fuchs, R., P. Male, and I. Mellman. 1989*a*. Acidification and ion permeabilities of highly purified rat liver endosomes. *J. Biol. Chem.* 264:2212–2220.

Fuchs, R., S. Schmid, and I. Mellman. 1989*b*. A possible role for Na^+ K^+-ATPase in regulating ATP-dependent endosome acidification. *Proc. Natl. Acad. Sci. USA.* 86:539–543.

Fushimi, K., J. A. Dix, and A. S. Verkman. 1990. Cell membrane fluidity in the intact kidney proximal tubule measured by orientation independent fluorescence anisotropy imaging. *Biophys. J.* 57:241–254.

Galloway, C. J., G. E. Dean, R. Fuchs, and I. Mellman. 1988. Analysis of endosome and lysosome acidification in vitro. *Methods Enzymol.* 157:601–611.

Gruenberg, J., and K. E. Howell. 1989. Membrane traffic in endocytosis: insights from cell-free assays. *Annu. Rev. Cell Biol.* 5:453–481.

Hopkins, C. R., A. Gibson, M. Shipman, and K. Miller. 1990. Movement of internalized ligand-receptor complexes by a continuous endosomal reticulum. *Nature (Lond.).* 346:335–339.

Inoue, S. 1989. Imaging of unresolved objects, superresolution and precision of distance measurement, with video microscopy. *In* Methods in Cell Biology. Vol. 30. D. L. Taylor and Y.-L. Wang, editors. 85–112.

Lencer, W. I., P. Weyer, A. S. Verkman, D. A. Ausiello, and D. Brown. 1990*a*. FITC-dextran as a probe for endosome function and localization in the kidney. *Am. J. Physiol.* 258:C309–C317.

Lencer, W. I., A. S. Verkman, D. A. Ausiello, A. Arnaout, and D. Brown. 1990*b*. Endocytic vesicles from renal papilla which retrieve the vasopressin-sensitive water channel do not contain an H^+ ATPase. *J. Cell Biol.* 111:379–389.

Mellman, I., R. Fuchs, and A. Helenius. 1986. Acidification of the endocytic and exocytic pathways. *Annu. Rev. Biochem.* 55:663–700.

Okhuma, S., Y. Moriyama, and T. Takano. 1982. Identification and characterization of a proton pump on lysosomes by fluorescein isothiocyanate-dextran fluorescence. *Proc. Natl. Acad. Sci. USA.* 79:2758–2762.

Park, C. H. 1988. The role of cAMP and calcium in the regulation of endocytosis in the proximal tubule of rabbit kidney. *FASEB Fed. Am. Soc. Exp. Biol. Journal Abstracts.* 2:A494. (Abstr.)

Rodman, J. S., L. Seidman, and M. G. Farquhar. 1986. The membrane composition of coated pits, microvilli, endosomes, and lysosomes is distincting in the rat kidney proximal tubule. *J. Cell Biol.* 102:77–87.

Roederer, M., R. Bowser, and R. F. Murphy. 1987. Kinetics and temperature dependence of exposure of endocytosed material to proteolytic enzymes and low pH: evidence for a maturation model for the formation of lysosomes. *J. Cell Physiol.* 131:200–209.

Sabolic, I., and G. Burkhardt. 1986. Characteristics of the proton pump in rat renal cortical endocytic vesicles. *Am. J. Physiol.* 250:F817–F826.

Sabolic, I., and G. Burkhardt. 1988. Proton ATPase in rat renal cortical endocytic vesicles. *Biochem. Biophys. Acta.* 937:398–410.

Shi, L.-B., and A. S. Verkman. 1989. Very high water permeability in vasopressin-dependent endocytic vesicles in toad urinary bladder. *J. Gen. Physiol.* 94:1101–1105.

Straubinger, R. M., D. Papahadjopoulos, and K. Hong. 1990. Endocytosis and intracellular fate of liposomes using pyranine as a probe. *Biochemistry.* 29:4929–4939.

Van Dyke, R. W. 1988. Proton pump-generated electrochemical gradients in rat liver multivesicular bodies: quantitation and effects of chloride. *J. Biol. Chem.* 263:2603–2611.

Verkman, A. S. 1989. Mechanisms and regulation of water permeability in renal epithelia. *Am. J. Physiol.* 257:C837–C850.

Verkman, A. S., and R. J. Alpern. 1987. Kinetic transport model for cellular regulation of pH and solute concentration in the renal proximal tubule. *Biophys. J.* 51:533–546.

Verkman, A. S., W. Lencer, D. Brown, and D. A. Ausiello. 1988. Endosomes from kidney collecting tubule contain the vasopressin-sensitive water channel. *Nature (Lond.).* 333:268–269.

Verkman, A. S., R. Takla, B. Sefton, C. Basbaum, and J. H. Widdicombe. 1989*a*. Quantitative fluorescence measurement of chloride transport in phospholipid vesicles. *Biochemistry.* 28:4240–4244.

Verkman, A. S., P. Weyer, D. Brown, and D. A. Ausiello. 1989*b*. Functional water channels are present in clathrin coated vesicles from bovine kidney but not from brain. *J. Biol. Chem.* 264:20608–20613.

Willingham, M. C., and I. Pastan. 1984. Endocytosis and exocytosis: current concepts of vesicle traffic in animal cells. *Int. Rev. Cytol.* 92:51–92.

Xie, X.-S., D. K. Stone, and E. Racker. 1983. Determinants of clathrin-coated vesicle acidification. *J. Biol. Chem.* 258:14834–14838.

Yamashiro, D. J., and F. R. Maxfield. 1987*a*. Kinetics of endosome acidification in mutant and wild-type Chinese hamster ovary cells. *J. Cell Biol.* 105:2713–2721.

Yamashiro, D. J., and F. R. Maxfield. 1987*b*. Acidification of morphologically distinct endosomes in mutant and wide-type Chinese hamster ovary cells. *J. Cell Biol.* 105:2723–2733.

Ye, R., L.-B. Shi, W. Lencer, and A. S. Verkman. 1989. Functional colocalization of water channels and proton pumps on endocytic vesicles from proximal tubule. *J. Gen. Physiol.* 93:885–902.